Permeability of Fluorescent Probes at Phase Transitions from Bilayer-coated Capsule Membranes[1]

Yoshio Okahata,* Naomi Iizuka, Gen-ichi Nakamura, and Takahiro Seki
Department of Polymer Science, Tokyo Institute of Technology, Ookayama, Meguro-ku, Tokyo 152, Japan

Ultrathin nylon capsule membranes coated with synthetic bilayers, the hydrophilic head groups of which carried cationic, anionic, and zwitterionic charges, were prepared. The bilayer-coated capsule membranes were used to measure the permeability of 13 water-soluble fluorescent probes, having cationic, anionic, zwitterionic, and non-ionic hydrophilic groups, across the membrane. A bilayer supported on a capsule membrane is more suitable for kinetic studies of permeation and trapping experiments than is a liposomal membrane. The permeability of fluorescent probes was drastically changed near a phase-transition temperature (T_c) of a coating bilayer, depending on the charges on the hydrophilic groups of both bilayers and permeant probes. From both activation energy data and shapes of Arrhenius plots, the permeation process of large probe molecules below and above the T_c is discussed, in comparison with that of a small electrolyte such as NaCl.

The ability of a lipid bilayer to act as an effective barrier to free solute diffusion and permeation has been assessed in various ways.[2,3] Liposomes have proved to be quite useful for this purpose, and in most studies on the permeability of bilayer vesicles the outward flow of entrapped material has been studied.[4–7] However, liposomes have some serious drawbacks for kinetic studies of permeability. Thus, (i) a bilayer wall may be too weak and fragile to withstand the osmotic pressure difference, (ii) a separation of the vesicles from all free solute is required by techniques such as dialysis, gel filtration, and membrane filtration, (iii) since the volume of the inner aqueous phase is very small, the encapsulation efficiency is low and high concentrations of substances are needed, and (iv) in studies of permeability as a function of temperature, vesicles are liable to fuse with each other in the phase-transition region. The strength of the bilayer wall has recently been improved by introducing various types of polymeric linkage.[8–17]

To overcome the problems of bilayer vesicles, we have prepared strong, ultrathin nylon capsule membranes, in which the nylon film is broken by a large number of pores which connect the outside to the inside of the capsule. These pores arise naturally during the formation of the capsules. The pores are then occluded with lipid bilayers, and we have studied the permeation of solutes across these bilayers from the inside to the outside of the capsule.[18–28] Permeation of NaCl across the bilayer-coated capsule membrane is affected by phase transitions of the coating bilayers like those of liposomes, and the permeation mechanism below and above T_c has been discussed in detail from the point of view of activation energy.[18–20,25] Since the bilayers supported on the capsule membrane are strong and still have characteristics of bilayer vesicles, they were expected to be suitable for kinetic studies of permeation.

In this article, we describe the permeation of 13 water-soluble fluorescent probes which have various kinds of hydrophilic group across the bilayer-coated capsule membrane in the phase transition region. In particular, the permeation mechanism, depending on hydrophilic groups of bilayers and permeants, is discussed in terms of activation energy data from Arrhenius plots, in comparison with that of a small electrolyte such as NaCl.

An illustration of a bilayer-coated capsule membrane, the apparatus for the permeation experiments, and structures of the bilayer-forming amphiphiles are shown in Scheme 1. Structures of water-soluble fluorescent probes used as permeants which can be trapped in the inner aqueous phase of the capsule are summarized in Figure 1.

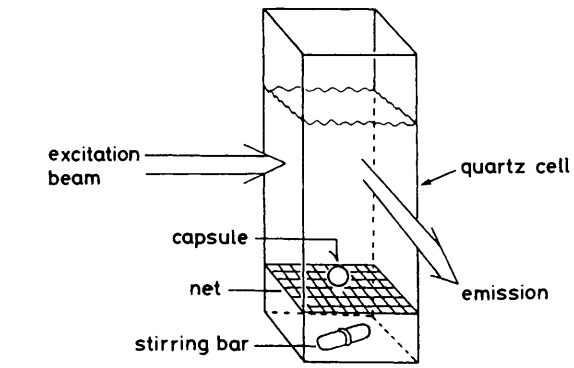

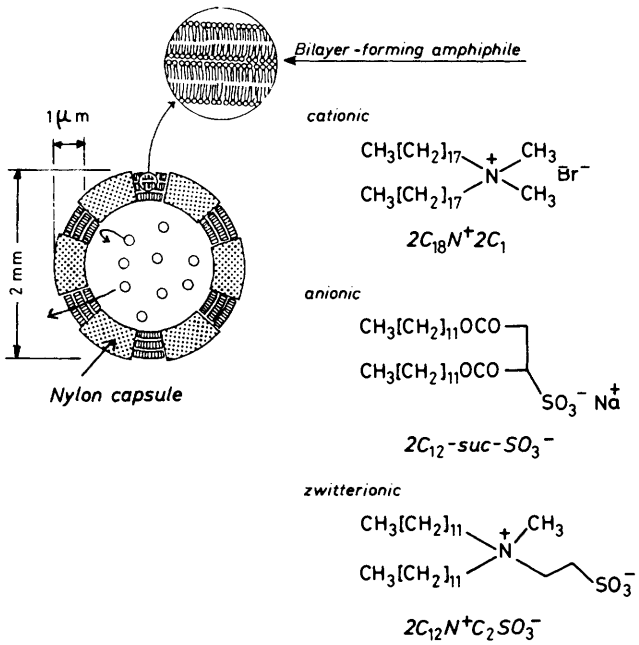

Scheme 1.

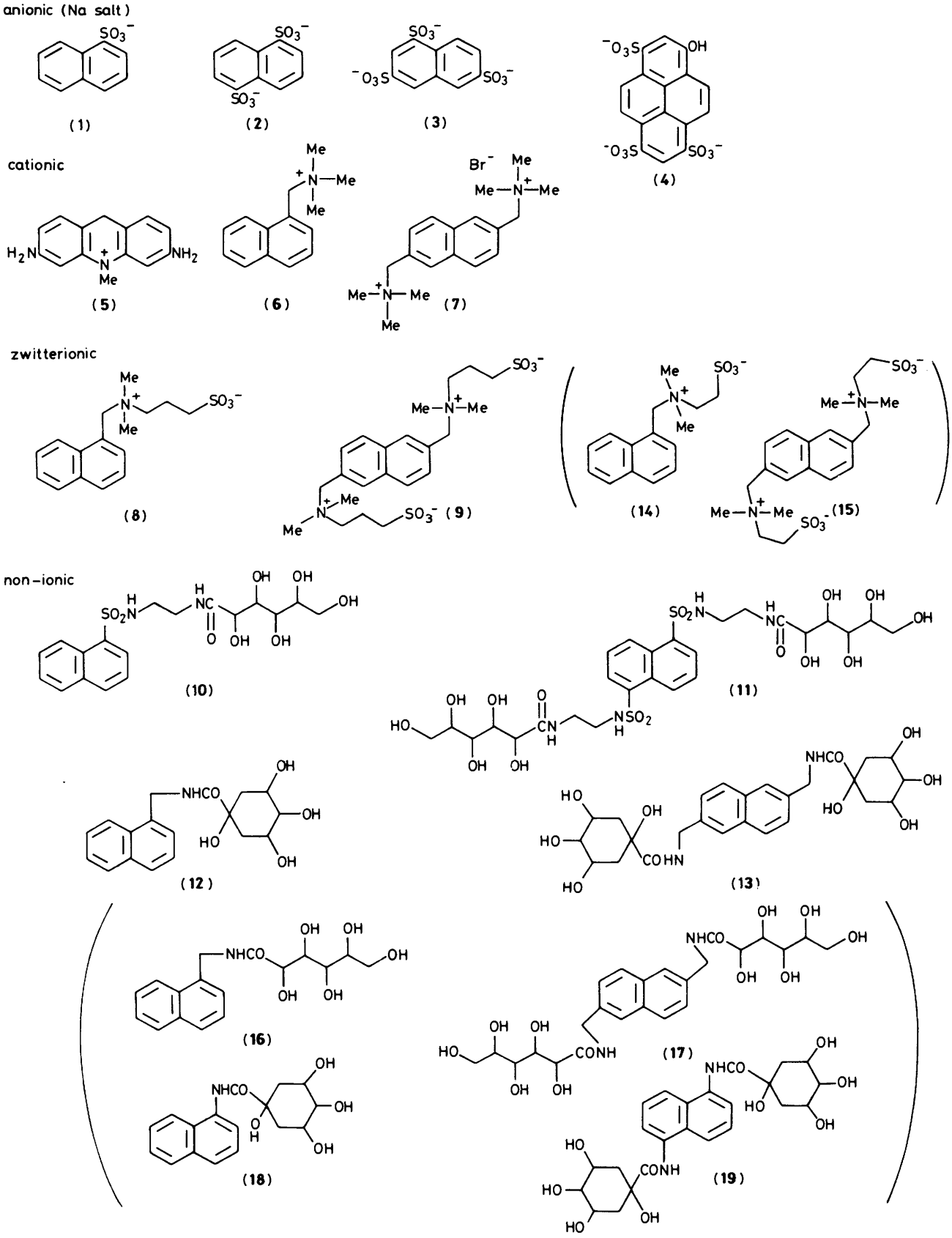

Figure 1. Structures of water-soluble fluorescent probes trapped in the inner aqueous phase of the capsule; probes in parentheses were not used as permeants because of low solubility in water

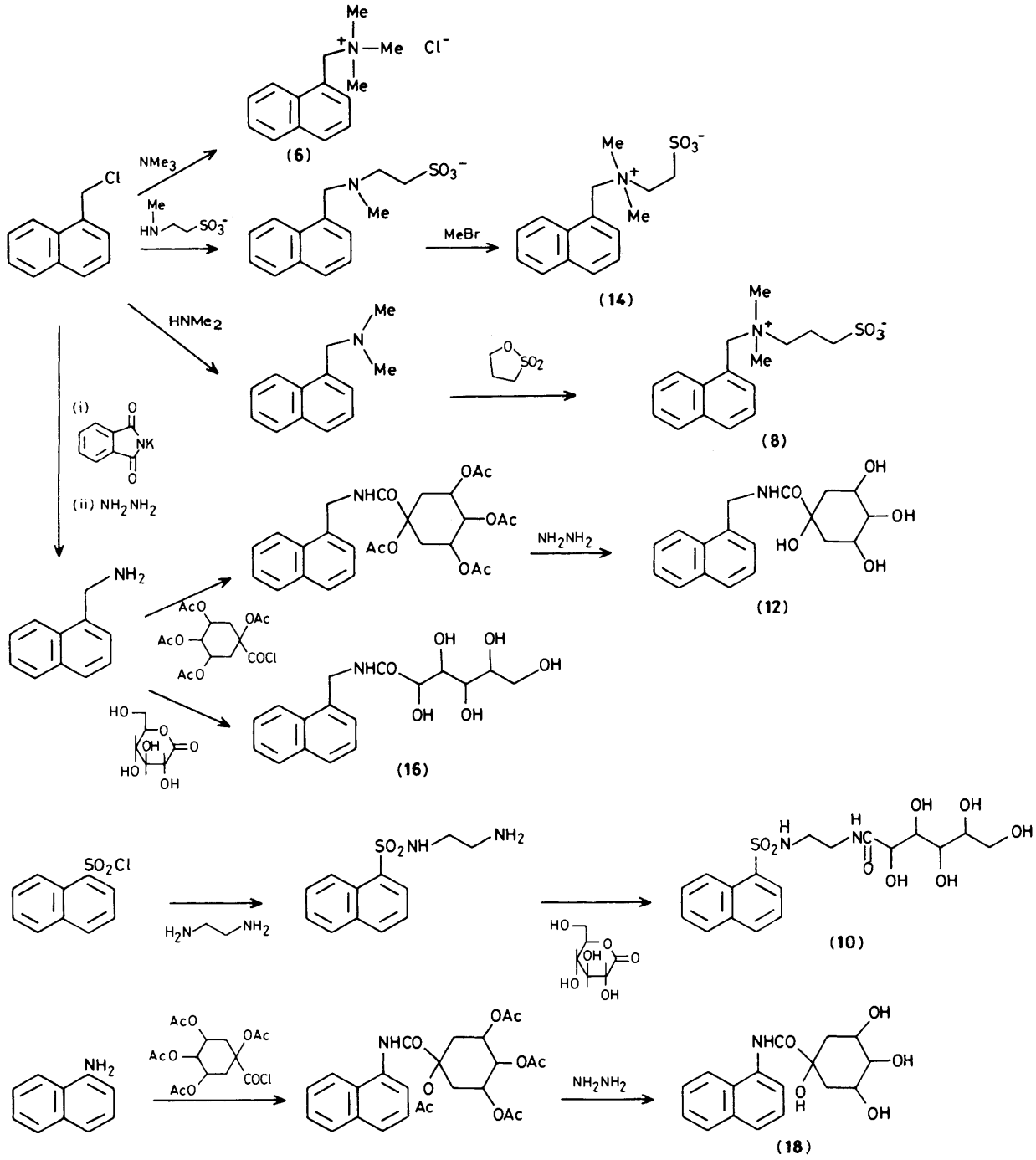

Scheme 2.

Experimental

Preparation of Fluorescent Probes.—Anionic fluorescent probes, sodium naphthalene-1-sulphonate (**1**), disodium naphthalene-1,5-disulphonate (**2**), trisodium naphthalene-1,3,6-trisulphonate(**3**),andtrisodium8-hydroxypyrene-1,3,6-trisulphonate (pyranine) (**4**), and the cationic 3,6-diamino-10-methylacridinium chloride (**5**) were purchased commercially (Tokyo Kasei Co, Japan) and further purified by recrystallization from aqueous acetone.

The synthetic routes to other cationic, zwitterionic, and nonionic fluorescent probes having one hydrophilic group are summarized in Scheme 2. Fluorescent probes having two hydrophilic groups were prepared by similar routes. The structures of the fluorescent probes obtained were confirmed by t.l.c. with a TF-10 flame-ionization detector (Iatoron Laboratories, Japan) and by i.r. and n.m.r. spectrometry, and by elemental analysis (C, H, and N).

Cationic fluorescent probes, 1-(trimethylammoniomethyl)-naphthalene chloride (**6**) and 2,6-bis(trimethylammoniomethyl)naphthalene dibromide (**7**), were prepared from 1-(chloromethyl)naphthalene (Tokyo Kasei Co, Japan) and 2,6-bis(bromomethyl)naphthalene[29,30] [m.p. 185 °C (from acetone)], respectively, with an excess of trimethylamine in dimethylformamide at 60 °C for 12—36 h. The monocationic

probe (**6**) formed white granules (98%), m.p. 252 °C. The dicationic probe (**7**) afforded white granules (from acetone–water) (72%), m.p. >300 °C.

The zwitterionic probe (**14**), in which a sulphonate group is linked to an ammonium group by a ethylene unit, was prepared as follows. 1-(Chloromethyl)naphthalene was treated with sodium *N*-methyltaurinate in the presence of Na_2CO_3 in ethanol for 3 days, and the product was quaternized with methyl bromide in H_2O–methanol at room temperature for 3 days to give white granules, m.p. 270—275 °C (from hot water) (2.4 g, 82%). The di-zwitterionic probe (**15**) was prepared from 2,6-bis(bromomethyl)naphthalene; m.p. >300 °C (from H_2O–methanol) (58%).

The other zwitterionic fluorescent probe (**8**), having a sulphopropyl-*N*,*N*-dimethylammoniomethyl group, was prepared as follows. 1-(Chloromethyl)naphthalene was treated with dimethylamine and the product was quaternized with propanesultone in ethanol for 24 h, giving white granules (from ethanol–water) (3.6 g, 37%), m.p. 251 °C. The di-zwitterionic probe (**9**) was prepared from 2,6-bis(dimethylaminomethyl)naphthalene (m.p. 97—99 °C) and propanesultone in the same manner as white granules (from ethanol–water) (3.4 g, 64%), m.p. 286 °C (decomp.)

The non-ionic fluorescent probe (**12**) having a hydrophilic quinamidomethyl group was prepared as follows. 1-(Aminomethyl)naphthalene (1.3 g, 8.3 mmol) obtained from 1-(chloromethyl)naphthalene by Gabriel synthesis was acylated with tetra-acetylquinoyl chloride[31,32] (3.4 g, 9 mmol) in chloroform and triethylamine (1.2 ml, 9.0 mmol) for 5 h under reflux conditions. The oily product was hydrolysed with an excess of hydrazine in EtOH–H_2O (1:1) at 90 °C for 1 day to give a white powder (from hot water), m.p. 169—171 °C (1.0 g, 36%).

2,6-Bis(quinamidomethyl)naphthalene (**13**) was prepared from 2,6-bis(aminomethyl)naphthalene (m.p. 148—151 °C) in a same manner as white plates, m.p. 222—227 °C (from MeOH–propan-2-ol) (0.7 g, 60%).

Other quinoyl-type fluorescent probes (**18**) and (**19**) were prepared *via* the acylation of 1-aminonaphthalene and 1,5-diaminonaphthalene, respectively, with tetra-acetylquinoyl chloride and subsequent hydrolysis: (**18**), m.p. 201—203 °C; (**19**) m.p. >300 °C.

Non-ionic fluorescent probes (**16**) and (**17**) having a gluconamide group were prepared from 1-(aminomethyl)naphthalene and 2,6-bis(aminomethyl)naphthalene, respectively, and gluconolactone in methanol under reflux for 3 h: (**16**), m.p. 170 °C (from hot water) (83%); (**17**), m.p. 250 °C (decomp.) (86%).

The non-ionic fluorescent probe (**10**) was prepared as follows. *N*-(β-Aminoethyl)naphthalene-1-sulphonamide (2.5 g, 10 mmol; m.p. 95—97 °C) obtained from naphthalene-1-sulphonyl chloride and ethylenediamine, was refluxed with gluconolactone (2.1 g, 12 mmol) in methanol for 12 h, giving white granules (from water) (3.0 g, 70%), m.p. 144—146 °C. A non-ionic probe having two gluconamide units, (**11**), was prepared from 2,6-bis-(*N*-β-aminoethylsulphamoyl)naphthalene in the same manner, giving white granules (from water) (1.8 g, 35%), m.p. 181—182 °C.

Preparation of Amphiphiles.—Preparations of dioctadecyldimethylammonium bromide ($2C_{18}N^+2C_1$), sodium didodecylsulphosuccinate ($2C_{12}$-*suc*-SO_3^-) and didodecylmethylammonioethanesulphonate ($2C_{12}N^+C_2SO_3^-$) are reported elsewhere.[25,33]

Preparation of Capsules.—Large Nylon-2,12 capsules were obtained from ethylenediamine and 1,10-bis(chlorocarbonyl)-decane by interfacial polymerization using a drop technique in the presence of a small amount of a cross-linking agent (trimesoyl chloride) according to previous methods.[18–20] Nylon capsules with an ultrathin membrane thickness of 1.0 ± 0.2 μm and a large diameter of 2.0 ± 0.1 mm were obtained. The nylon capsule was found to have small numbers of residual CO_2H and NH_2 end groups (*ca.* 1×10^{-4} equiv. g^{-1}) by acid–base titration.[26] In order to avoid the effect of ionization of these groups, the residual end groups were changed to CO_2Me and NHAc groups by methylation (MeOH–H_2SO_4) and acylation (Ac_2O), respectively. The content of residual end groups was confirmed to be less than 1×10^{-5} equiv. g^{-1} by acid–base titration. The capsules with blocked end groups were dialysed against aqueous 0.01M-phosphate buffer (pH 7) containing an appropriate fluorescent probe (1×10^{-3}M) to give capsules containing probe molecules.

Amphiphile-coated capsules were prepared as follows:[18–20] twenty pieces of capsule containing fluorescent probes were transferred to a dodecane solution (3 ml) of dialkyl amphiphile (50 mg) and maintained at 60 °C for 5 min. After being cooled, the amphiphile-coated capsules were picked up, rolled on filter paper to remove the excess of dodecane solution, and kept in aqueous solution containing 1×10^{-3}M-fluorescent probe. The amphiphile content on the capsule was 20 ± 3 μg per capsule, and dodecane was confirmed not to be an impurity in the coating amphiphiles by elemental analysis.

Measurements.—Differential scanning calorimetry (DSC) of coating amphiphiles was carried out with a Perkin-Elmer DSC-2 instrument. Five crushed, bilayer-coated capsules were sealed with 10 μl of water in a sample pan and heated from 5 to 90 °C at 10 °C per min.

Fluorescence anisotropy of fluorescent probes was measured in both aqueous solution and aqueous vesicle solution of corresponding amphiphiles, using polarizer and analyser plates. The steady-state anisotropy ratio r_s was calculated from equation (1) for linearly polarized excitation, where $I_{\parallel}$ and $I_{\perp}$

$$r_s = (I_{\parallel} - G\,I_{\perp})/(I_{\parallel} - 2G\,I_{\perp}) \quad (1)$$

are the components of emission polarized parallel and perpendicular to the excitation polarization direction, and G is the ratio of sensitivities of the detection system for vertically and horizontally polarized light, obtained from $G = I_{vert.}/I_{hor.}$, with horizontally polarized excitation.[34,35]

Permeation of capsules towards the fluorescent probe trapped in the inner aqueous phase was followed by detecting increases in the relative fluorescence intensity of the outer water phase, after dropping one capsule into 3 ml of deionized water in a quartz cell (see apparatus in Scheme 1).

Results

Characterization of Amphiphiles on the Capsule Membrane.—The large, ultrathin nylon capsule membrane (diameter 2 mm, membrane thickness 1 μm) was prepared and the pores in it were occluded with amphiphiles from the interface of dodecane and water. It has been reported that amphiphiles exist as multiple-bilayer structures on the porous capsule membrane by *X*-ray analysis and electron microscopy.[18–20,25] This was also proved for the cationic $2C_{18}N^+2C_1$, the anionic $2C_{12}$-*suc*-SO_3^-, and the zwitterionic $2C_{12}N^+C_2SO_3^-$ amphiphile-coated capsule membranes used in this study. Thus, *X*-ray analysis of the bilayer-coated capsule showed strong reflections with 30—40 Å spacing, consistent with the bimolecular length of the amphiphiles (the incident beam was exposed perpendicular to the intersection of the capsule membrane). In transmission electron microscopy, an enlargement of a favourable area of the ultrathin piece of bilayer-coated capsule membrane (stained negatively by uranyl acetate) showed the distinct multi-lamellar structure, the mean thickness of which is estimated to be

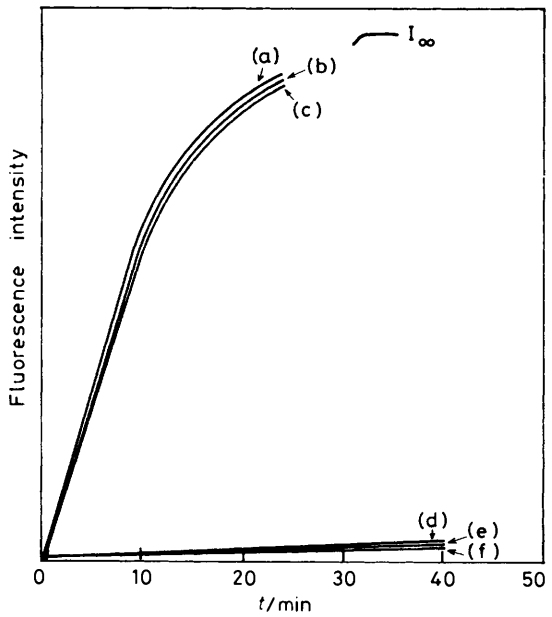

Figure 2. Course of permeations of anionic fluorescent probes across the uncoated capsule membrane [curves (a)—(c)] and the $2C_{12}$-*suc*-SO_3^- bilayer-coated capsule membrane [curves (d)—(f)] at 45 °C; (a) and (d) monoanionic probe (**1**), (b) and (e) dianionic probe (**2**), (c) and (f) trianionic probe (**3**)

30—40 Å, depending on the alkyl chain length of the amphiphile. These results clearly indicate that the coating amphiphiles (cationic $2C_{18}N^+2C_1$, anionic $2C_{12}$-*suc*-SO_3^- and zwitterionic $2C_{12}N^+C_2SO_3^-$) exist as a multi-lamellar structure growing parallel to the membrane plane (illustrated in Scheme 1), like capsules coated with phospholipids[20] and other bilayer-forming amphiphiles.[25]

The liquid crystalline property is one of the fundamental physicochemical characteristics of synthetic dialkyl bilayers[33] as well of phospholipids. In differential scanning calorimetry, all the amphiphiles on the capsule membrane showed a sharp endothermic peak, which indicates a phase transition from crystal to liquid crystalline state, similar to that shown in aqueous vesicle dispersions. The observed phase-transition temperatures (T_c) were as follows: cationic $2C_{18}N^+2C_1$, 45 °C; anionic $2C_{12}$-*suc*-SO_3^-, 60 °C; zwitterionic $2C_{12}N^+C_2SO_3^-$, 56 °C.

Fluorescent Probes.—All of the anionic [(**1**)—(**4**)] and cationic [(**5**)—(**7**)] fluorescent probes obtained were freely soluble in aqueous solution. Some non-ionic and zwitterionic fluorescent probes (shown in parentheses in Figure 1), however, showed poor solubility in water. Zwitterionic probes having one or two ammonioethylsulphonate groups [(**14**) and (**15**)] were completely insoluble in water, probably because of the formation of tight intramolecular ion-pairs, in contrast to zwitterionic probes containing ammoniopropanesulphate groups [(**8**) and (**9**)]. Non-ionic fluorescent probes having gluconamide units as hydrophilic groups [(**16**) and (**17**)] were not sufficiently soluble in water; however, probes (**10**) and (**11**), having both sulphonamide and gluconamide units, were freely soluble in water. 1-(Quinamido)naphthalene (**18**) and 2,6-bis(quinamido)-naphthalene (**19**) were insoluble in water, in contrast to the (quinamidomethyl)naphthalenes (**12**) and (**13**).

In the following permeation experiments, four anionic (**1**)—(**4**), three cationic (**5**)—(**7**), two zwitterionic (**8**) and (**9**), and four non-ionic fluorescent probes (**10**)—(**13**), which were freely soluble in water, were used as permeants (see Figure 1).

Permeation of Fluorescent Probes.—Permeation of fluorescent probes through the capsule membrane was followed by detecting increases in the fluorescence intensity of the outer water phase after dropping one capsule into the distilled water, as shown in the apparatus of Scheme 1. The fluorescent probes released to the outer phase were excited at 280 nm for (**1**)—(**3**) and (**6**)—(**13**), at 408 nm for (**4**), and at 456 nm for (**5**), and the fluorescence was monitored at 340, 510, and 504 nm, respectively. Typical time courses of permeations of anionic fluorescent probes across capsule membranes at 45 °C are shown in Figure 2. Apparent permeation rates P were calculated from the initial slopes in Figure 2 using equation (2),[18—20,25]

$$P = kd/6I_\infty \quad (2)$$

where k and d are the increase in the fluorescence intensity with time (the slope of Figure 2) and the capsule diameter, respectively; I_∞ was measured as the fluorescence intensity after the capsule had been crushed to release its contents to the bulk solution. From I_∞ values, the concentrations of fluorescent probes trapped in the inner aqueous phase of both uncoated and bilayer-coated capsules were estimated to be $(1.0 \pm 0.1) \times 10^{-3}$M, nearly equal to that of the dialysis solution (1.0×10^{-3}M).

When the uncoated capsule membrane was employed, all probes were completely released within 10 min [P = (3—5) $\times 10^{-5}$ cm s^{-1}]. The nylon capsule expanded slightly during the experiment and reverted slowly to its original size after complete release of probes. This is because the nylon capsules are made of a semipermeable, porous membrane, and water (P = *ca.* 10^{-3} cm s^{-1}) can permeate much faster than probes across membranes. A similar phenomenon was also observed in NaCl release from the uncoated capsule.[18] When the capsule was coated with anionic $2C_{12}$-*suc*-SO_3^- bilayers, a marked decrease in the anionic probe efflux was observed and the capsule scarcely expanded, unlike the uncoated capsule. This indicates that the anionic bilayer coats are impermeable to both water and anionic fluorescent probes.

Permeation rates at 45 °C of cationic, anionic, zwitterionic, and non-ionic fluorescent probes across the capsule membrane coated with positively and negatively charged and neutral (zwitterionic) bilayers were obtained from equation (2) and are summarized in Table 1. Permeation of all probes through the uncoated capsule membrane was very fast, regardless of charge and hydrophilicity of probes [(2.9—5.7) $\times 10^{-5}$ cm s^{-1}]. The permeability of probes through the bilayer-coated capsule membrane largely depended on both the surface charge on the coating bilayer and the hydrophilic group of the permeant. When the capsule was coated with negatively charged $2C_{12}$-*suc*-SO_3^- and positively charged $2C_{18}N^+2C_1$ bilayers, the permeation of anionic [(**1**)—(**4**)] and cationic [(**5**)—(**7**)] probes was markedly reduced, relative to the uncoated capsule. Charged bilayer coats also showed greatly reduced permeability toward disubstituted neutral probes [(**9**), (**11**), and (**13**)]. Capsules coated with zwitterionic $2C_{12}N^+C_2SO_3^-$ bilayers were permeable to most probes except dianionic (**2**), trianionic (**3**), and dicationic probes (**7**). Permeability through the hydrophobic bilayer coats was generally reduced with increasing hydrophilicity (the number of hydrophilic substituents) of permeants. The electrostatic repulsion between bilayers and probes seems also to be important.

With combinations of cationic bilayer coatings and anionic probes (**1**)—(**4**), and of anionic bilayer-coatings and cationic probes (**5**)—(**7**), strange permeation behaviour was observed and a permeation rate was not obtained, probably because of interaction between oppositely charged probes and amphiphiles (Table 1). In order to clarify the extent of interactions between probes and surface charges on bilayers, the fluorescence

Table 1. Permeation rates of fluorescent probes across capsule membranes at 45 °C

	10^7 (P/cm s^{-1})			
Permeants	Uncoated	$2C_{12}$-*suc*-SO_3^--coated	$2C_{18}N^+2C_1$-coated	$2C_{12}N^+C_2SO_3^-$-coated
Monoanionic (**1**)	540	0.17	*a*	51
Dianionic (**2**)	420	0.085	*a*	1.7
Trianionic (**3**)	390	0.018	*a*	0.18
Pyranine (**4**)	310	0.010	*a*	
Acridinium (**5**)	410	*a*	0.10	
Monocationic (**6**)	570	*a*	10	70
Dicationic (**7**)	510	*a*	9.8	3.5
Mono-zwitterionic (**8**)	560	17	60	68
Di-zwitterionic (**9**)	290	2.1	0.93	51
Mono-non-ionic (**10**)	510	2.0	9.4	75
Di-non-ionic (**11**)	310	0.35	1.5	62
Mono-non-ionic (**12**)	490	13	24	
Di-non-ionic (**13**)	290	0.75	2.5	

[a] Permeation rates could not be obtained because of the formation of hydrophobic ion-pairs between probes and bilayer coats.

Table 2. Fluorescence anisotropy of probes in anqueous dispersions of bilayer vesicles at 25 °C[a]

	10^3 r_s			
Fluorescent probes	In water	$2C_{12}$-*suc*-SO_3^- vesicles	$2C_{18}N^+2C_1$ vesicles	$2C_{12}N^+C_2SO_3^-$ vesicles
Monoanionic (**1**)	1.22	0.583	29.3	1.28
Pyranine (**4**)	5.33	4.96	40.7	2.85
Acridinium (**5**)	3.29	33.9	2.56	4.17
Dicationic (**7**)	0.695	24.8	2.20	0.951
Mono-zwitterionic (**8**)	6.26	7.91	12.6	11.0
Mono-non-ionic (**10**)	4.05	4.99	4.48	3.80

[a] Obtained from equation (1); [probe] = 1.0×10^{-5} M, [amphiphile] = 1.0×10^{-4} M

anisotropy (r_s) of the probes was measured in aqueous solution both in the presence and in the absence of bilayer vesicles of $2C_{18}N^+2C_1$, $2C_{12}$-*suc*-SO_3^-, and $2C_{12}N^+C_2SO_3^-$ [equation (1); see Experimental section]. The results are summarized in Table 2. Anionic and cationic probes gave remarkably high r_s values only in aqueous dispersions of negatively and positively charged vesicles. In the absence of an electrostatic interaction between probes and surface charges of bilayers, the same range of r_s values was observed as in water. This indicates that only the charged probe binds strongly to the oppositely charged bilayers by electrostatic interaction. Hence the strange permeation behaviour was observed only in the combination of oppositely charged probes and bilayer-coated capsules. Thus, in most of other cases, in the absence of the electrostatic interaction between probes and bilayers, probes seem to be trapped in the inner aqueous pool of capsules without interacting with the surface charge of bilayer coats, and will permeate the hydrophobic bilayers.

Effect of Temperature; Arrhenius Plots.—Since the coating bilayers on the capsule membrane show the phase-transition phenomenon, as well as aqueous dispersion of liposomes and synthetic bilayer vesicles, the permeation of fluorescent probes through the membrane is expected to be affected by the phase transitions of the coating bilayers. Permeation rates of bilayer-coated capsule membranes towards 13 fluorescent probes were obtained in the phase-transition temperature region (40—75 °C). Arrhenius plots of the permeation of anionic probes (**1**)—(**4**) and neutral probes (**8**)—(**13**) through the capsule membrane coated with the anionic $2C_{12}$-*suc*-SO_3^- bilayers (T_c 60 °C) are shown in Figures 3 and 4, respectively. Figures 5 and 6 show Arrhenius plots of the permeation of cationic probes (**5**)—(**7**) and neutral probes (**10**) and (**11**) through the cationic $2C_{18}N^+2C_1$ bilayer coatings (T_c 45 °C), respectively. Arrhenius plots of the capsule coated with the zwitterionic $2C_{12}N^+C_2SO_3^-$ bilayers (T_c 56 °C) are shown in Figure 7.

In the case of the uncoated capsule, permeations of all probes had nearly the same rates and gave simple, straight Arrhenius plots, unaffected by variation of the hydrophilic substituents. However, for most bilayer-coated capsule membranes, Arrhenius plots showed a break near the phase-transition temperature (T_c) of the coating bilayer (separately obtained by DSC measurements and shown by arrows in the Figures). The slopes of the two straight lines intersecting near T_c and the magnitudes of the permeation rates depend both on surface charges of the bilayer coats and on the hydrophilicity of the permeating probes. Permeation of ionic probes through charged bilayers generally gave a sharply inflected Arrhenius plot near T_c, in which the slope below is usually steeper than above T_c (Figures 3 and 5). With neutral (zwitterionic and non-ionic) probes permeating through charged bilayer coats, only the highly hydrophilic probes having two substituents gave a sharply inflected Arrhenius plot (Figures 4 and 6). In the permeation of less hydrophilic probes having single substituents, however, Arrhenius plots gave only slight changes in slope at T_c; permeability was scarcely reduced below or above T_c. In the case of zwitterionic bilayer coats, only the highly hydrophilic trianionic probe (**3**) gave a sharply inflected Arrhenius plot (Figure 7). This means that charged bilayers are less permeable to a hydrophilic probe than neutral (zwitterionic) bilayers, owing to electrostatic repulsion between matrix and permeants.

Activation energies for permeation obtained from slopes of

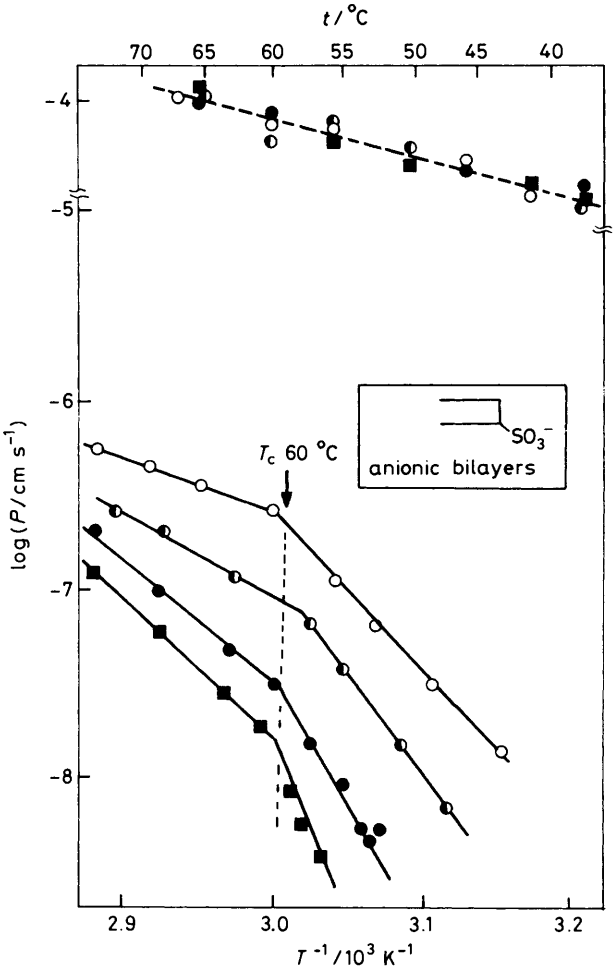

Figure 3. Arrhenius plots of the permeation of monoanionic probe (**1**) (○), dianionic probe (**2**) (◐), trianionic probe (**3**) (●) and pyranine (**4**) (■) through the anionic $2C_{12}$-*suc*-SO_3^- bilayer-coated capsule. The dotted lines in this and following Figures show the Arrhenius plots of the uncoated capsule. Values of T_c of the coating bilayers are shown by an arrow

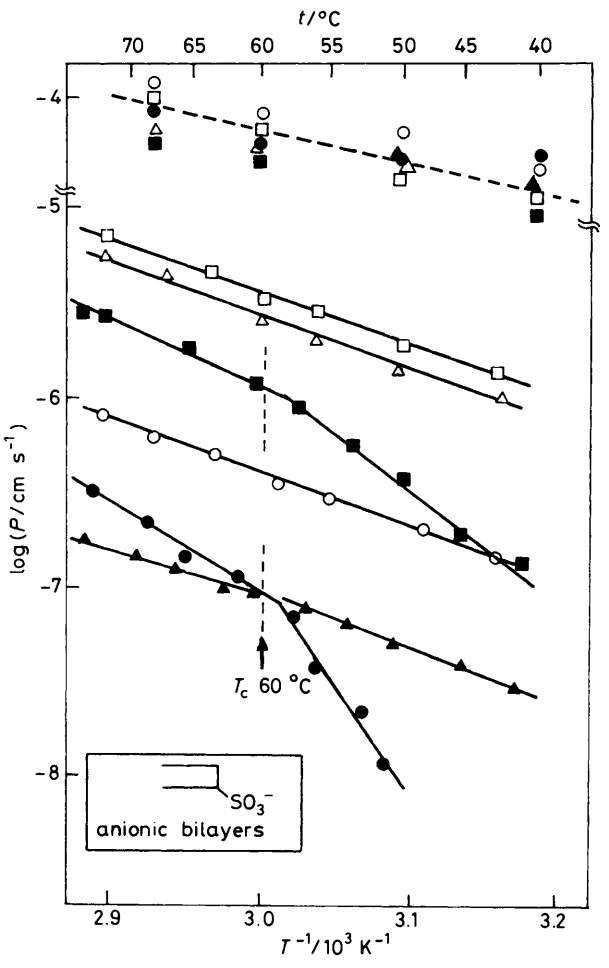

Figure 4. Arrhenius plots of the permeation of mono-zwitterionic probe (**8**) (□), di-zwitterionic probe (**9**) (■), mono-non-ionic probes (**10**) (○) and (**12**) (△), and di-non-ionic probes (**11**) (●) and (**13**) (▲) through the anionic $2C_{12}$-*suc*-SO_3^- bilayer-coated capsule

Arrhenius plots both below and above T_c are summarized in Table 3, together with those for NaCl permeation across bilayer-coated capsules.[25]

Discussion

From the Arrhenius plots, we can deduce that the permeability is greatly affected by the phase transitions of the coating bilayers; it is much less in the solid-like state below T_c when the highly hydrophilic probe permeates the bilayer-coated capsules. When relatively large molecules such as water-soluble naphthalene derivatives diffuse and permeate through ordered bilayers, the lipid matrix around a permeant particle becomes disordered, causing a high activation energy which depends on the extent of rigidity. The permeation of anionic probes (**1**)—(**4**) through the negatively charged $2C_{12}$-*suc*-SO_3^--bilayers gave higher activation energies (42—110 kcal mol^{-1})* in the solid-like state below T_c than in the liquid-like state above T_c (13—32 kcal mol^{-1}) (Table 3). Values of E_a increase with the hydrophilicity of permeants in the order mono-, di-, and tri-sulphonate both below and above T_c (Figure 3). Increases of E_a values were usually more rapid in the solid-like state below T_c than above T_c. Thus, the larger permeants such as pyranine (**4**) gave higher E_a values, particularly in the rigid gel state below T_c. Similar trends in E_a values were also observed in the permeation of cationic probes (**5**)—(**7**) through the positively charged $2C_{18}N^+2C_1$ bilayers (Figure 5 and Table 3).

The trends in E_a values can be explained as follows. For the permeation of these relatively bulky molecules (in comparison with electrolytes such as NaCl and water molecules), the rate-limiting step may be the penetration to the ordered bilayers. The rate of penetration into the hydrophobic matrix, disturbing the ordered lipid, depends on both the hydrophilicity and on the bulkiness of the permeant, and the effect should be observed more clearly in the solid-like state below T_c than in the liquid-like state above T_c. Thus the permeation of pyranine (**4**), having a large pyrene unit and three sulphonate groups, through the rigid bilayers below T_c, gives a high E_a value (110 kcal mol^{-1}). Although it is difficult to compare directly with data for permeation data through liposomal membranes, we note that E_a values for the permeation of dyes such as Phenol Red and dansylgalactoside through pure phospholipid bilayers (small uni-lamellar and large multi-lamellar vesicles) have been reported to be 20—30 kcal mol^{-1} above and 150—300 kcal mol^{-1} below the phase transition.[6,7]

In some cases of permeation of monosubstituted non-ionic and zwitterionic probes through charged bilayers, and in most

*1 cal = 4.184 J.

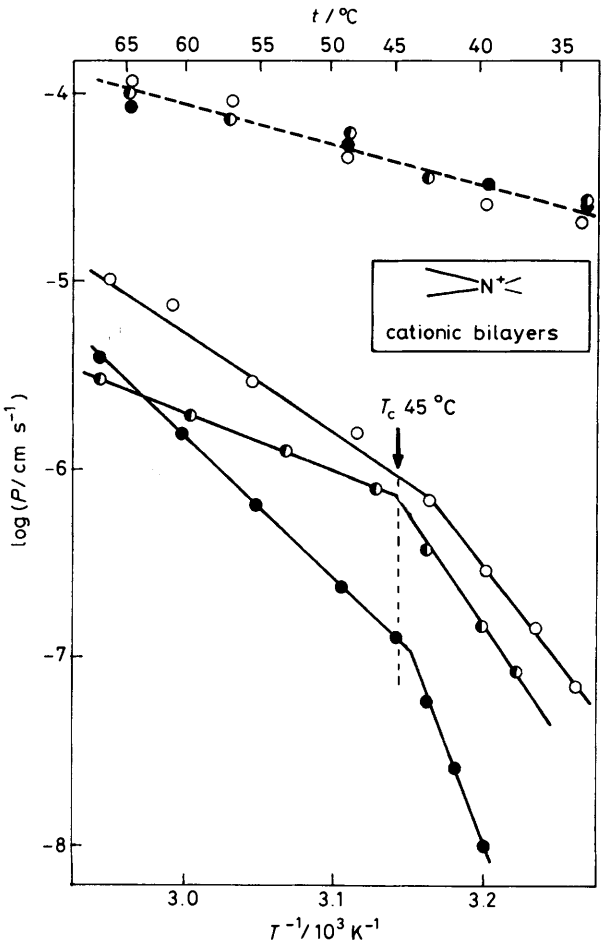

Figure 5. Arrhenius plots of the permeation of acridinium (**5**) (●), monocationic (**6**) (○) and dicationic (**7**) (◐) probes through the cationic $2C_{18}N^+2C_1$ bilayer-coated capsule

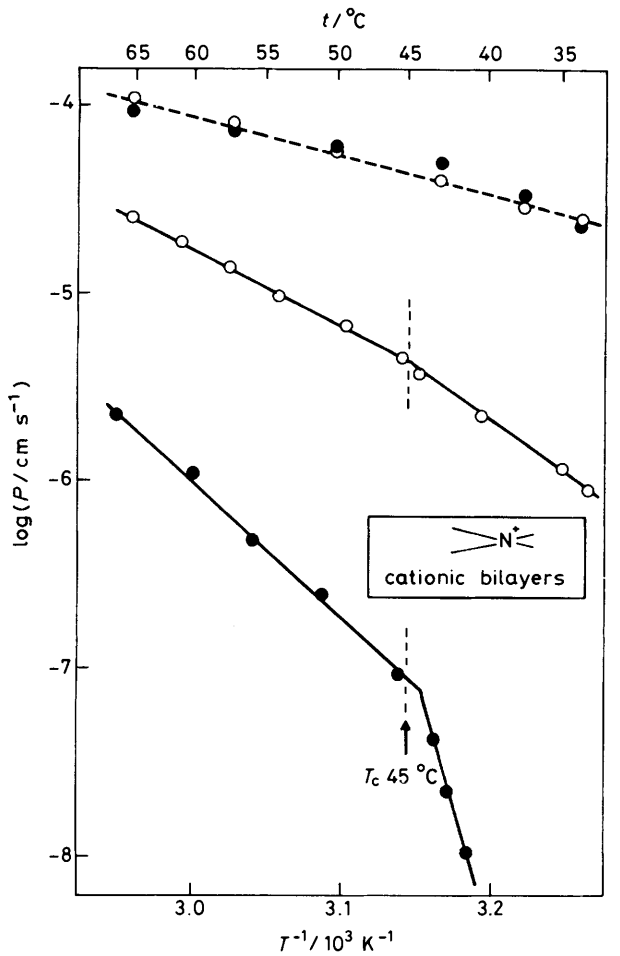

Figure 6. Arrhenius plots of the permeation of mono-non-ionic (**10**) (○) and di-non-ionic (**11**) (●) probes through the cationic $2C_{18}N^+2C_1$ bilayer-coated capsule membrane

Table 3. Activation energy data on fluorescent probe permeation across capsule membranes

	E_a/kcal mol^{-1} [a]						
		$2C_{12}$-*suc*-SO_3^--coated		$2C_{18}N^+2C_1$-coated		$2C_{12}N^+C_2SO_3^-$-coated	
Probes	Uncoated	Below T_c	Above T_c	Below T_c	Above T_c	Below T_c	Above T_c
NaCl [b]	5.5	3.8	14	4.1	5.5	5.9	19
Monoanionic (**1**)	12	42	13			10 [c]	
Dianionic (**2**)	9.5	51	19			31	20
Trianionic (**3**)	9.9	64	28			62	22
Pyranine (**4**)	10	110	32				
Acridinium (**5**)	8.9			46	15		
Monocationic (**6**)	8.5			42	26	11 [c]	
Dicationic (**7**)	7.6			73	35	28	19
Mono-zwitterionic (**8**)	15	13 [c]					
Di-zwitterionic (**9**)	13	27	16				
Mono-non-ionic (**10**)	11	13 [c]		24 [c]			
Di-non-ionic (**11**)	8	51	19	90	33		
Mono-non-ionic (**12**)	10	12 [c]					
Di-non-ionic (**13**)	10	30	18				

[a] 1 kcal = 4.148 kJ. [b] See ref. 25. [c] Arrhenius plots were hardly inflected at T_c

cases of permeations of ionic probes through zwitterionic bilayers, Arrhenius plots did not show a marked inflection, and relatively small E_a values (10—19 kcal mol^{-1}) were obtained (see Figures 4, 6, and 7). The monosubstituted probe seems to be less hydrophilic and penetrates more easily into the hydrophobic matrix, giving smaller E_a values than di- or tri-substituted probes. This is more clearly observed in the permeation through zwitterionic $2C_{12}N^+C_2SO_3^-$ bilayers in the absence of charge

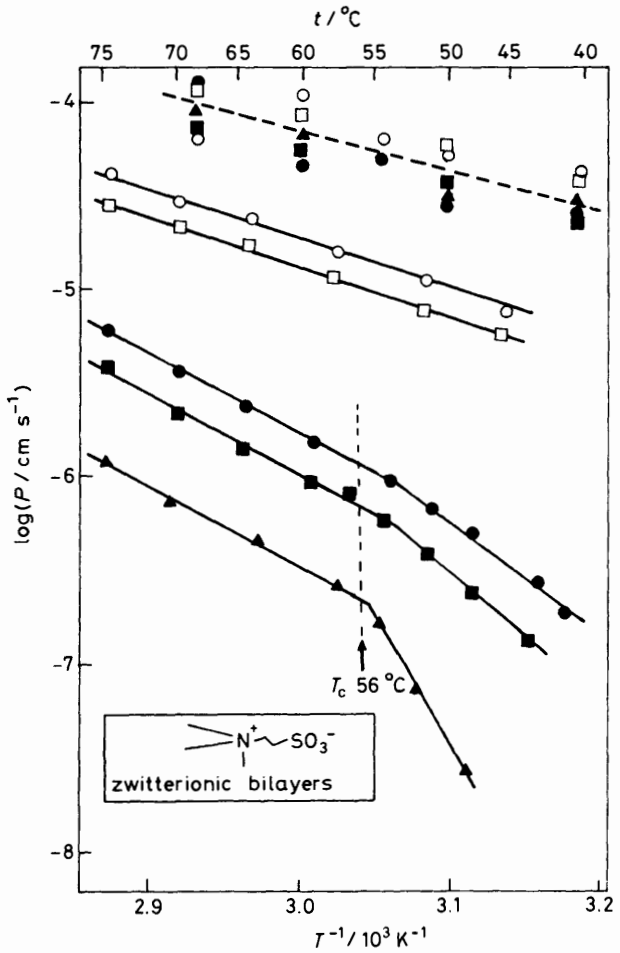

Figure 7. Arrhenius plots of the permeation of monoanionic probe (**1**) (□), dianionic probe (**2**) (■), trianionic probe (**3**) (▲), monocationic probe (**6**) (○), and dicationic probe (**7**) (●) through the zwitterionic $2C_{12}N^+C_2SO_3^-$ bilayer-coated capsule membrane

repulsion between permeants and the bilayer matrix, than in the permeation of ionic probes through charged bilayers. The highly hydrophilic probe (**3**) gave a higher E_a value (62 kcal mol^{-1}) below T_c than above T_c (22 kcal mol^{-1}).

In the permeation of these large fluorescent probe molecules, the perturbation of boundary lipids around a permeant becomes important relative to the dehydration process. In the rigid gel state below T_c, the permeant must disturb a large number of lipid molecules. The resulting very high activation energy must be exactly compensated by the melting entropy; hence the Arrhenius plots are continuous, and inflected at the phase transition.

Another type of Arrhenius plot, causing a disruption at the phase transition, has been observed in the permeation of small electrolytes such as NaCl through bilayer-coated capsule membranes; their Arrhenius plots are illustrated in Figure 8.[18,20,25] In this case a different mechanism is proposed. In the permeation of Na^+ and Cl^- through a hydrophobic bilayer matrix, dehydration of the permeant should be important since the permeant is very small and highly hydrated. As a bilayer system resembles a more structured system than the surrounding water, the transfer of Na^+ and Cl^- into this hydrophobic barrier will be accompanied by a unfavourable entropy change. This decrease in entropy is expected to be smaller for penetration into a liquid-like membrane than into a solid-like membrane. These differences result in a discontinuity in the

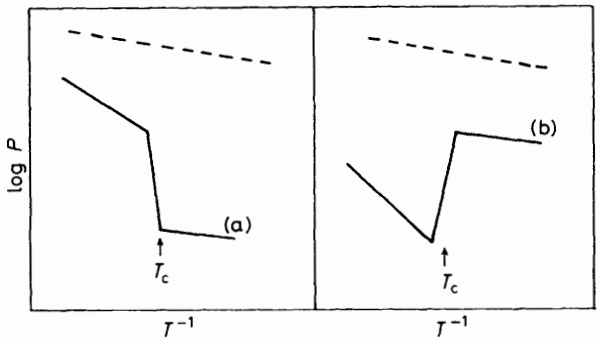

Figure 8. Schematic illustrations of Arrhenius plots of NaCl permeation across the capsule membrane coated with (a) charged bilayers [cationic $2C_nN^+2C_1$, (n = 12—18) or anionic $2C_{12}$-*suc*-SO_3^-] and (b) neutral charged bilayers (zwitterionic $2C_{12}N^+C_2SO_3^-$ or $2C_{16}$-PC).[18-20,25] Dotted lines show Arrhenius plots of the uncoated capsule

Arrhenius plots at T_c (Figure 8). Above T_c, NaCl permeates through the fluid though hydrophobic bilayer matrix with a relatively high E_a value (5.5—19 kcal mol^{-1}; Table 3).[25] In the rigid gel state, small ions can be released through interstices or pores in the coating multi-lamellar bilayers. Values of E_a below T_c, then, become lower (3.8—5.9 kcal mol^{-1}) and similar to those of the uncoated capsule (E_a 5.5 kcal mol^{-1}), in which NaCl permeation proceeds simply by a diffusion process.

Two different types of Arrenius curve (*a* and *b* in Figure 8) have been observed in NaCl permeation. Positively or negatively charged bilayers on the capsule contain few defective pores in the gel state, and permeability below T_c is quite low relative to that above T_c (curve *a* in Figure 8).[18] However, neutral (zwitterionic and non-ionic) bilayer-coatings easily produce small defective pores in the gel state, and NaCl permeation below T_c is not greatly reduced relative to that of the uncoated capsule (curve *b*). Since these defective pores disappear in the fluid, liquid crystalline state of bilayer-coatings above T_c, NaCl permeation is drastically decreased above T_c, with high E_a values, because of permeation through the fluid hydrophobic matrix.[25] In the permeation of fluorescent probes through the zwitterionic bilayer matrix, however, anomalous permeation behaviour depending on the surface charge of the bilayer coatings was not observed (Figure 7). This is because large molecules such as these fluorescent probes cannot pass through the small defective pores in rigid bilayers, and must diffuse, disturbing the ordered rigid bilayers with a very high E_a value.

Different types of Arrhenius plots depending on permeants have also been reported for liposomal membranes:[2-7] the permeation of smaller molecules such as sugars or metal ions gives disruption with or without maximum at the phase transition in Arrhenius plots, and in the case of larger molecules such as a dye, the Arrhenius plot is only inflected at T_c (as in the fluorescent probe permeation of the present study).

Conclusions

The permeation of 13 fluorescent probes through cationic, anionic, and zwitterionic bilayers supported on a nylon capsule membrane has been studied in the phase-transition region. Permeability is greatly affected both by surface charges on the bilayer coats and by the hydrophilicity of the permeants, especially in the solid-like state below T_c of the bilayers. The permeation process for the large probe molecules seems to be different in type from that of a small electrolyte, giving a large activation energy for permeation through the solid-like bilayers. Since the bilayer structure supported on the capsule membrane

is strong and still has characteristics of bilayers (although multiple), it may become a new tool for kinetic studies of permeation and trapping experiments.

References

1 This is Part 15 of the series 'Functional Capsule Membranes;' for Part 14, see ref. 27.
2 D. Papahadjopourous, K. Jacobson, S. Nir, and T. Isac, *Biochim. Biophys. Acta*, 1973, **311**, 330.
3 R. A. Demel, S. C. Kinsky, C. B. Kinsky, and L. L. M. van Deenen, *Biochim. Biophys. Acta*, 1968, **150**, 655.
4 S. C. Kinsky, in 'Methods in Enzymology,' vol. 32, eds. S. Fleischer and L. Packer, Academic Press, New York, 1977, pp. 501—513.
5 G. J. M. Bresseleers, H. Goderis, and P. P. Tobback, *Biochim. Biophys. Acta*, 1984, **772**, 374.
6 F. Jahnig, and J. Bramhall, *Biochim. Biophys. Acta*, 1980, **690**, 310.
7 L. F. Braganza, B. H. Blott, T. J. Coe, and D. Melville, *Biochim. Biophys. Acta*, 1983, **731**, 137.
8 T. Kunitake, N. Nakashima, K. Takarabe, M. Nagai, A. Tsuge, and H. Yanagi, *J. Am. Chem. Soc.*, 1981, **103**, 5945.
9 P. Tundo, D. J. Kippenberger, P. L. Klahn, N. E. Prieto, T. C. Jad, and J. H. Fendler, *J. Am. Chem. Soc.*, 1982, **104**, 456.
10 W. Reed, L. Gutterman, P. Tundo, and J. H. Fendler, *J. Am. Chem. Soc.*, 1984, **106**, 1897.
11 S. L. Regen, A. Singh, G. Oehme, and M. Singh, *J. Am. Chem. Soc.*, 1982, **104**, 791.
12 H. H. Hub, B. Hupfer, H. Koch, and H. Ringsdorf, *J. Macromol. Sci., Chem.*, 1981, **15**, 701.
13 D. F. O'Brien, T. H. Whitesides, and R. T. Klingbiel, *J. Polym. Sci., Polym. Lett. Ed.*, 1981, **19**, 95; K. Dorn, R. T. Klingbiel, D. P. Specht, P. N. Tyminski, H. Ringsdorf, and D. F. Brien, *J. Am. Chem. Soc.*, 1984, **106**, 1627.
14 L. Gros, H. Ringsdorf, and H. Schupp, *Angew. Chem., Int. Ed. Engl.*, 1981, **20**, 305.
15 M. F. M. Roks, H. G. J. Visser, J. W. Zwikker, A. J. Verkley, and R. J. M. Nolte, *J. Am. Chem. Soc.*, 1983, **105**, 4506.
16 J. H. Fendler and P. Tundo, *Acc. Chem. Res.*, 1984, **17**, 3.
17 S. L. Regen, J. S. Shin, and K. Yamaguchi, *J. Am. Chem. Soc.*, 1984, **106**, 2446.
18 Y. Okahata, S. Hachiya, and G. Nakamura, *Chem. Lett.*, 1982, 1719; Y. Okahata, H.-J. Lim, G. Nakamura, and S. Hachiya, *J. Am. Chem. Soc.*, 1983, **105**, 4855.
19 Y. Okahata, H.-J. Lim, and S. Hachiya, *Makromol. Chem. Rapid Commun.*, 1983, **4**, 303; *J. Chem. Soc., Perkin Trans. 2*, 1984, 989.
20 Y. Okahata, H.-J. Lim, and G. Nakamura, *Chem. Lett.*, 1983, 755; Y. Okahata and H.-J. Lim, *J. Am. Chem. Soc.*, 1984, **106**, 4696.
21 Y. Okahata and H. Noguchi, *Chem. Lett.*, 1983, 1517.
22 Y. Okahata, G. Nakamura, S. Hachiya, H. Noguchi, and H.-J. Lim, *J. Chem. Soc., Chem. Commun.*, 1983, 1206.
23 Y. Okahata, K. Ozaki, and T. Seki, *J. Chem. Soc., Chem. Commun.*, 1984, 519.
24 Y. Okahata, S. Hachiya, and T. Seki, *J. Chem. Soc., Chem. Commun.*, 1984, 1337.
25 Y. Okahata, H.-J. Lim, and G. Nakamura, *J. Membr. Sci.*, 1984, **19**, 237.
26 T. Seki and Y. Okahata, *Macromolecules*, 1984, **17**, 1880.
27 Y. Okahata and T. Seki, *Chem. Lett.*, 1984, 1261; *J. Am. Chem. Soc.*, 1984, **106**, 8065.
28 Y. Okahata, S. Hachiya, and T. Seki, *J. Polym. Sci., Polym. Lett. Ed.*, 1984, **22**, 595.
29 W. Baker, F. Glockling, and J. F. W. McOmie, *J. Chem. Soc.*, 1951, 1118.
30 W. Ried and H. Bodem, *Chem. Ber.*, 1958, **91**, 1981.
31 Y. Murakami, A. Nakano, J. Kikuchi, and T. Takaki, *Chem. Lett.*, 1983, 1891.
32 R. Grewe and H. Haendler, *Justus Liebigs Ann. Chem.*, 1962, **658**, 113.
33 Y. Okahata, R. Ando, and T. Kunitake, *Ber. Bunsenges. Phys. Chem.*, 1981, **85**, 789.
34 K. Kano and J. H. Fendler, *Biochim. Biophys. Acta*, 1978, **509**, 289.
35 T. Seki, J. Komiyama, T. Iijima, and U. P. Wild, *Colloid Polym. Sci.*, 1984, **262**, 311.

Received 6th *November* 1984; *Paper* 4/1892